CONFOCAL MICROSCOPY

ALBERTO DIASPRO
FEDERICO FEDERICI
University of Genoa
Genoa, Italy
MARIO FARETTA
IFOM-IEO Campus for Oncogenomics
Milan, Italy
CESARE USAI
National Research Council
Genoa, Italy

1. INTRODUCTION

In modern times, there is an increasing demand for three-dimensional (3-D) optical microscopy (1,2). The main reason lies in the fact that optical microscopy is still unique in its ability to allow the complete three-dimensional examination of biological structures in a hydrated state under experimental conditions that allow the preservation of living or physiological states, also when compared with other high-resolution techniques (3). This fact coupled with the advent of fluorescence labeling permits the study of the complex and delicate relationships existing between structure and function in biological systems. One relevant step, in terms of progress in 3-D optical microscopy, was the invention of the confocal microscope in its different solutions (4). Minsky, in 1957, invented a confocal microscope identical with the concept later developed extensively by Egger and Davidovits at Yale, by Sheppard and Wilson at Oxford, and by Brakenhoff et al. in Amsterdam (5). It was in the mid-1970s, with the advent of affordable computers and lasers, and the development of digital image processing software, that the first confocal laser scanning microscopes became available in several laboratories and applied to biological and material specimens (6–9).

2. THREE-DIMENSIONAL OPTICAL SECTIONING

It is a matter of fact that the possibility of a 3-D reconstruction of an object starting from the acquisition of two-dimensional (2-D) datasets, i.e., 2-D optical slices, is one of the most powerful procedures for morphological analysis and volume rendering, especially within biological sciences where the opportunity for optical slicing allows one to get information from different planes of the specimen without being invasive, thus preserving structures and functionality.

When a set of 2-D images is acquired at various focus positions and under certain conditions, in principle, one can recover the 3-D shape of the object. Unluckily, the observed image $o(x, y, z)$, produced by the true intensity distribution $i(x, y, z)$, is corrupted by the characteristic transfer function, i.e., point spread function (PSF), of the image formation system $s(x, y, z)$, by additive noise stemming from different sources $n(x, y, z)$ and by cross-information coming from different planes rather than from the focus one.

At a certain plane of focus z_0 within the sample or, optical sectioning along the z-axis, at a plane j over N within the 3-D sample, the observed image can be regarded as the following (10):

$$o_j = i_j \otimes s_0 + \sum_{k \neq j} i_k \otimes s_k + n, \tag{1}$$

where the subscripts on i and o refer to the discretized z plane, whereas the subscripts on s refer to the number of the k-plane away from the "in-focus" position at the actual jth plane.

This relationship is usually transferred to the Fourier frequency domain, where the convolution operator becomes an algebraic multiplication. Image restoration algorithms (deconvolution) aim to invert such equations to extract the true measured quantity $i(x, y, z)$, thus allowing a 3-D sample reconstruction directly by piling up 2-D images, after further scale correction is performed, accounting for axial distortion phenomena linked to the refractive index mismatch. The solution of the problem is simplified when operating under the so-called confocal scheme (4,11).

The confocal scheme is essentially based on an automatic fine z-stepping either of the objective or of the sample stage, coupled with the usual x-y point-to-point scanning of the focal plane and image capturing. The synchronous x-y-z scanning allows the collection of a set of in-focus two-dimensional images, which is less affected by signal cross-talk from other planes from the sample as more strictly confocality conditions are respected.

From Equation 1, ideally one gets

$$o_j = i_j \otimes s_0 + n. \tag{2}$$

Unfortunately, with respect to the wide-field conventional optical sectioning scheme, the confocal one requires a longer time for the image formation process because it uses a point-like scanning of the sample.

3. CONFOCAL PRINCIPLE AND LASER SCANNING MICROSCOPY

When thinking of conventional wide-field microscopes, one figures out some specimen entirely bathed in the radiation from the light source, viewed directly by eyes or through any capture device [charge-coupled device (CCD) camera, for instance] or photosensitive film. This means that samples undergo full excitation on every instant, leading to in- and out-of-focus light points contribution overlapping, worsening axial resolution, and producing that typical hazing in the collected images that, together with the light-diffraction effects, limits the instrument performances.

In contrast with this, the image formation in any confocal setup is intrinsically different (4,11).

The most important feature in confocal microscopy is the capability of discriminating between different focal planes and collecting the signal selectively from a plane of focus from within a sample. This naturally leads to an

Wiley Encyclopedia of Biomedical Engineering, edited by Metin Akay
ISBN 0-471-24967-X

improvement of the system performances because fine details are often scarcely detected in conventional non-confocal fluorescent microscopes.

This goal is achieved via two principal mechanisms that are at the basis of a point-to-point scanning of the selected plane of focus within the sample:

1. Incident light is focused to a spot (much smaller than the usual field of view) within the specimen through a very small aperture (*pinhole*). The benefits of such a focusing technique lie on the possibility of limiting the excitation of fluorescent dies above and below the plane of focus.
2. Light emission from regions above and below the considered plane of focus is physically blocked from reaching the detector by means of a second pinhole (or of the same one, depending on the architecture of the system).

These mechanisms are often referred as the "confocal principle" (Fig. 1).

To acquire an image, the excitation light has to be fully delivered to each point of the sample and the emission signal collected and displayed.

This is usually accomplished by means of two possible different strategies.

The first one is based on the sample scanning in a raster pattern such that, over every fixed period of time, the necessary amount of information from the focal plane is collected and the emitted light signal, usually detected through a photomultiplier tube (PMT), is displayed by the mapping of each single-point light emission. Sometimes the use of a one-direction moving slit (rather than a single point) is preferred for speeding up the scanning rate despite that this leads to an evident worsening of the spatial resolution and of the 3-D imaging capability.

A second possible approach to forming confocal images consists of employing a multi-pinhole Nipkow spinning disk, which is a disk containing multiple sets of spirally arranged pinholes placed in the image plane of the objective lens. A large parallel beam of light is then pointed to a particular region of the disk, and the lights passing through the illuminated pinholes are focused by the objective lens straight onto the specimen. When spinning the disk at a rapid rate, the sample may undergo excitation several hundred times per second: Emitted light is collected and imaged typically by a high-resolution and high quantum efficiency CCD camera. One meaningful advantage in the approach with respect to the previous one is an improvement of time resolution without compromising resolution.

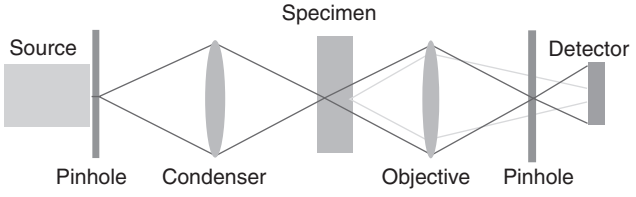

Figure 1. A simplified sketch of the confocal principle: Red rays are the confocal ones, whereas yellow rays show the optical pathway of contributions coming from adjacent "not-in-focus" planes. (This figure is available in full color at http://www.mrw.interscience.wiley.com/ebe.)

As for what concerns optical sectioning, every architecture is built such that the sample is placed along the light-path at a conjugate focal plane and the movements along the optical axis keep the focus at a fixed distance from the objective, making it possible to effectively scan different fields of view through the specimen (thanks to a step-to-step motor device attached to the fine focus) and collect a series of in-focus optical slices for 3-D reconstruction.

The degree of confocality is readily a function of the pinhole size: The use of smaller pinholes improves the discrimination of focused light from stray one, thus involving a thinner plane in the image formation process and improving resolution, at the cost of a lower light throughput, which makes things difficult when dealing with particularly dim samples.

In these architectures, z-resolution and optical sectioning thickness (which are basically the parameters involved in every optical sectioning process), depend on several factors such as the numerical aperture (NA) of the objective lens, the wavelength of the excitation/emission light, the pinhole size, the refractive index of components along the light path, and least but not last the overall alignment of the instrument.

4. THEORETICAL ANALYSIS

The development of an effective theoretical model for describing the properties of an optical system needs some preliminary, *realistic* assumptions to be done to simplify calculations.

Under this point of view, the use of a linear space invariant (LSI) model reveals itself as a good one, pliable enough to get important insights and develop suitable mathematical tools for the analysis of most concrete situations.

Let us consider the confocal cartoon in Fig. 2. A point monochromatic light source is focused onto some sample focal plane "j" through a lens L_1 (condenser), and the emitted radiation from the sample (which is supposed to be monochromatic too) is collected through a second lens L_2 (objective) by a point detector.

Let h_{ex} and h_{em} be, respectively, the transfer function of L_1 and L_2, i.e., the lens response to an input light point source. h_{ex} and h_{em} coincide with s_0 at the focal plane.

Under this hypothesis, it can be written that

$$U_{ex}(x) = (h_{ex} \otimes \delta_s)(x) = h_{ex}(x), \tag{3}$$

where the excitation light source is modeled by Dirac's impulse.

It can be shown that, being U_{ex} the signal reaching the sample, the emitted signal scales with the fluorescent dyes density D (D can be also extended to any other intensity property of the sample) according to the law:

$$U_{em} = D \cdot U_{ex}. \tag{4}$$

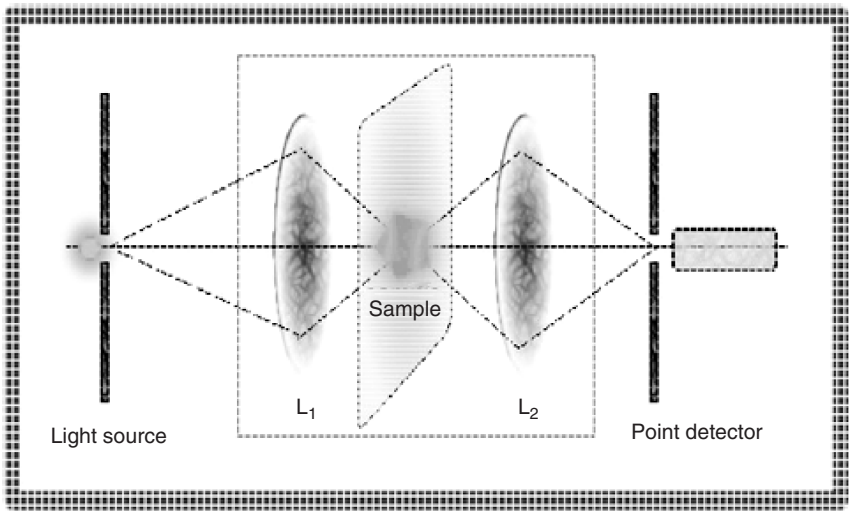

Figure 2. Cartoon of an equivalent optical setup for modeling image formation when using a confocal scheme. (This figure is available in full color at http://www.mrw.interscience.wiley.com/ebe.)

The emitted radiation is then focused on the point detector through L_2. This leads to

$$U_{\text{det}}(x) = ((h_{em} \otimes U_{em}) \cdot \delta_d)(x), \tag{5}$$

where the point detector function is assumed to be Dirac's impulse.

The overall signal collected by the detector, i.e., more generally the "observed image," is thus

$$\begin{aligned} I_{tot} &= \int U_{\text{det}}(x)dx = \int dx\delta_d(x)(h_{em} \otimes U_{em})(x) \\ &= \int dx\delta_d(x) \int dy h_{em}(x-y)D(y)h_{ex}(y) \\ &= \int dy D(y)h_{ex}(y) \int dx\delta_d(x)h_{em}(x-y) \\ &= \int dy D(y)h_{ex}(y)h_{em}(-y). \end{aligned} \tag{6}$$

If now we limit ourselves to a point-like sample,

$$\int U_{\text{det}}(x)dx = \int dy\delta(y)h_{ex}(y)h_{em}(-y) = h_{ex}(0)h_{em}(0), \tag{7}$$

where $h_{ex} = h_{em}$ under the hypothesis of $L_1 = L_2$ and $\lambda_{\text{ex}} = \lambda_{\text{em}}$.

As an *x*-*y*-*z* scanning process is generally coupled to the imaging one, it is natural to write, for a general point $P(x, y, z)$,

$$I_{tot} = h^2(x,y,z), \tag{8}$$

which is the general expression for the PSF, i.e., the system impulse response.

A mathematical expression for $h(x,y,z)$ can be obtained through the electromagnetic waves scalar theory (12). The formulation, lying on Frauenhofer diffraction, leads to

$$h(u,v) \propto \left| \int_0^1 J_0(v\rho)e^{-0.5iu\rho^2}\rho d\rho \right|^2, \tag{9}$$

where u and v are suitable dimensionless variables defined according to the following:

$$\begin{aligned} u &\propto z, \\ v &\propto \sqrt{x^2+y^2}. \end{aligned} \tag{10}$$

By limiting us to the points, respectively, along the optical axis and in the focal plane:

$$h(0,v) \propto \left[\frac{2J_1(v)}{v}\right]^2 \quad h(u,0) \propto \left(\frac{\sin(u/4)}{u/4}\right)^2 \tag{11}$$

that implies

$$I_{tot}(0,v)\left[\frac{2J_1(v)}{v}\right]^4 \quad I_{tot}(u,0) = \left(\frac{\sin(u/4)}{u/4}\right)^4. \tag{12}$$

As for conventional microscopes,

$$I_{tot} \approx h(u,v), \tag{13}$$

the evaluation of the FWHM (full-width at half-maximum), accounting for the system resolution, leads to a resolution improvement by a factor a 1.4, which turns into a factor of 3 in terms of volume.

Comparisons between the ideal PSF in the case of strict confocality with that of conventional microscopes may somehow account for resolution improvements, despite

Table 1. Values of Theoretical and Experimental FWHM of Confocal PSFs Using Different Pinhole Sizes

Oil (n = 1.52)	Lateral (nm) Pinhole 20 μm	Lateral (nm) Pinhole 50 μm	Axial (nm) Pinhole 20 μm	Axial (nm) Pinhole 50 μm
	186 ± 6	215 ± 5	489 ± 6	596 ± 4
Theoretical	*180*	*210*	*480*	*560*

the use of this mathematical formalism in concrete situations needs some further drawbacks to be highlighted.

First of all, there is a natural dependence between the pinhole size and the PSF: The more the pinhole size is increased, the more the confocal microscope's response tends to fit conventional ones.

This means that in the case of dim or high photosensitive specimens, some compromise has to be found between the resolution and the amount of the collected signals, according to the kind of analysis one is going to perform (whether a morphometric one or an intensity one).

Second, the PSF is obviously dependent on all other physical parameters such as the sample immersion medium refractive index and turbidity, the degree of homogeneity of the sample, and the photochemical properties of the used dyes. That is why the development of complicated computations often leads to poorly applicable results in practice because conditions are on every time.

One of the most meaningful PSF-dependences is that from the refractive index mismatch between the objective immersion medium and that from the sample solution.

Table 1 reports the value of theoretical and experimental FWHM of confocal PSFs using different pinhole sizes (13). A sample of subresolved bead (Polyscience, $\emptyset = (0.064 \pm 0.009)\,\mu m$) has been imaged by means of a 100X NIKON oil-immersion objective (NA = 1.3; WD = 20 mm) under Argon laser excitation ($\lambda = 488$ nm).

As one can see from the reported values, the system resolution is worse along the optical axis and is strictly dependent on the degree of confocality (pinhole size). Pinhole size is strongly architecture dependent. In the case reported here, the small size is related to the ideal condition discussed in the optical sectioning paragraph. The larger size, which is twice the small one, simply allows getting more light (useful in case of low fluorescence) at the expenses of resolution and optical sectioning ability. A large pinhole lets more intensity contributions coming from adjacent planes to pass to the detector.

The typical trends of the PSFs are reported in Fig. 3, where a comparison between experimental points and theoretical ones is possible: The evident asymmetry of the plots in the real case is somehow a typical one and

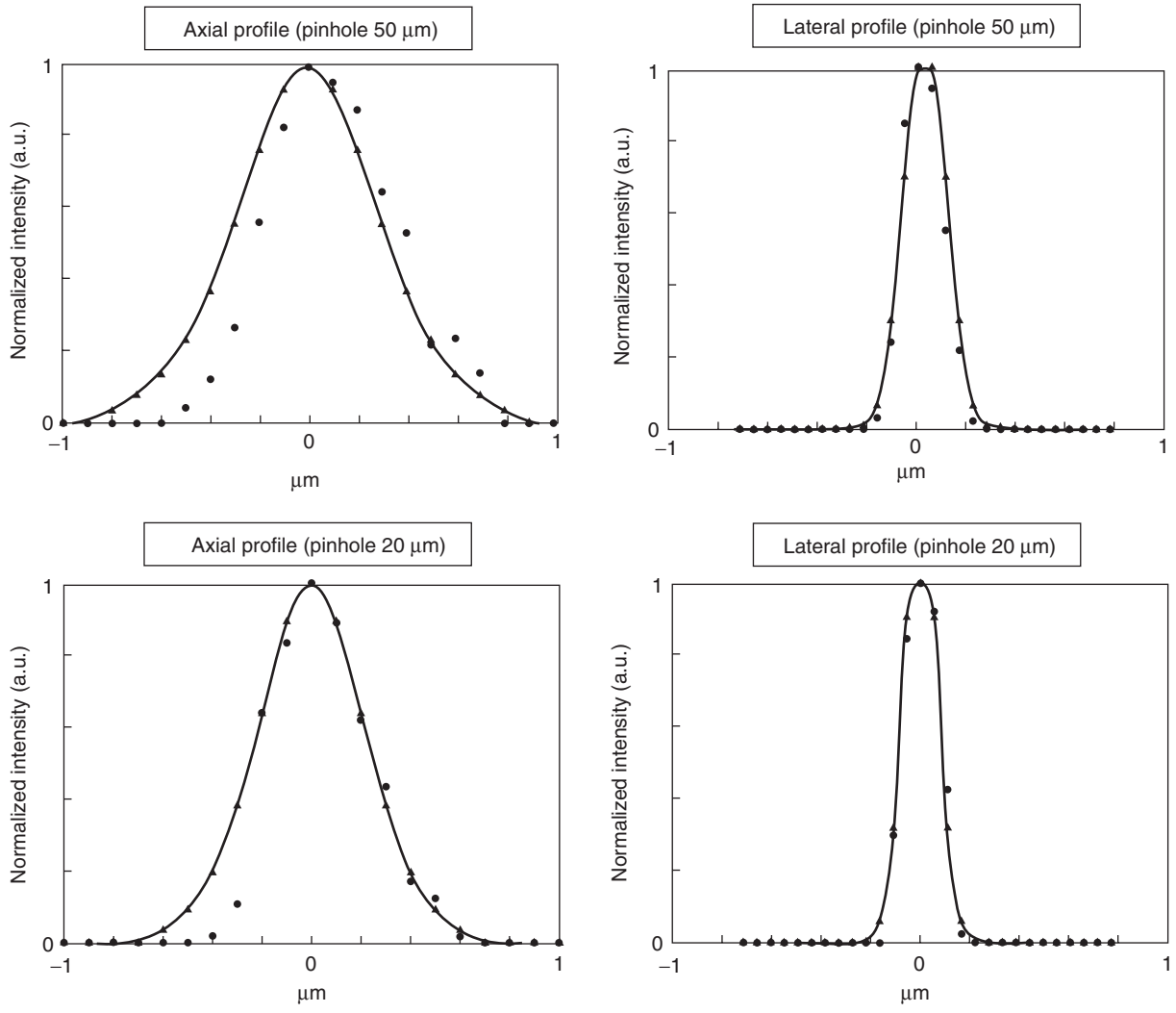

Figure 3. Experimental (dark dots) and theoretical (dark triangle) PSFs at various pinhole sizes.

Table 2. Variations of the Lateral and Axial FWHM PSH Value, with respect to the Focusing Depth

	Air		Glycerol		Oil	
Depth (μm)	Lateral (nm)	Axial (nm)	Lateral (nm)	Axial (nm)	Lateral (nm)	Axial (nm)
0	187±8	484±24	183±14	495±29	186±6	489±6
30	244±10	623±9	221±5	545±12	197±10	497±21
60	269±11	798±10	252±7	628±9	186±12	496±19
90	277±5	1063±24	268±8	797±26	191±9	484±12

Table 3. Typical Observed Values of the Percentage of Variation of the PSF Intensity Peak Under Different Mismatch Conditions and at a Different Focusing Depth

Medium	% at 30-μm Depth	% at 60-μm Depth	% at 90-μm Depth
Oil	3	6	7
Glycerol	17	27	34
Air	44	51	60

becomes even more evident when focusing through different stratified media.

The theory, developed within the contest of electromagnetic waves focusing across stratified media, suggests a progressive broadening of the PSF with respect to the focusing depth, becoming even more noticeable under refractive-index mismatch conditions (14).

As a consequence, the largest percentage of variation of the lateral FWHM, with respect to the focusing depth, swings from 6% (oil-immersed PSF) to 48% (air-immersed PSF), whereas the axial FWHM varies up to 130% (air-immersed PSF) (see Table 2).

This phenomenon goes with a subsequent weakening of the signal with respect to the focusing depth, which turns out to be more evident in the case of refractive-index mismatch.

Table 3 reports typical observed values of the percentage of variation of the PSF intensity peak under different mismatch conditions and at a different focusing depth (referred to as the coverslip).

Figure 4 shows a set of optical slices acquired by means of a confocal scheme. The images are reported without any processing demonstrating the 3-D optical sectional ability of the setup.

5. APPLICATIONS

The 3-D ability of the confocal scheme coupled to the natural property of fluorescence optical microscopy to allow imaging of living samples moves the imaging scenario in a four-dimensional world (*x-y-z-t*), where other dimensions can be added and other mechanisms of fluorescence excitation can be considered, like multiphoton excitation [7, and this book]. So far, it is difficult to report about

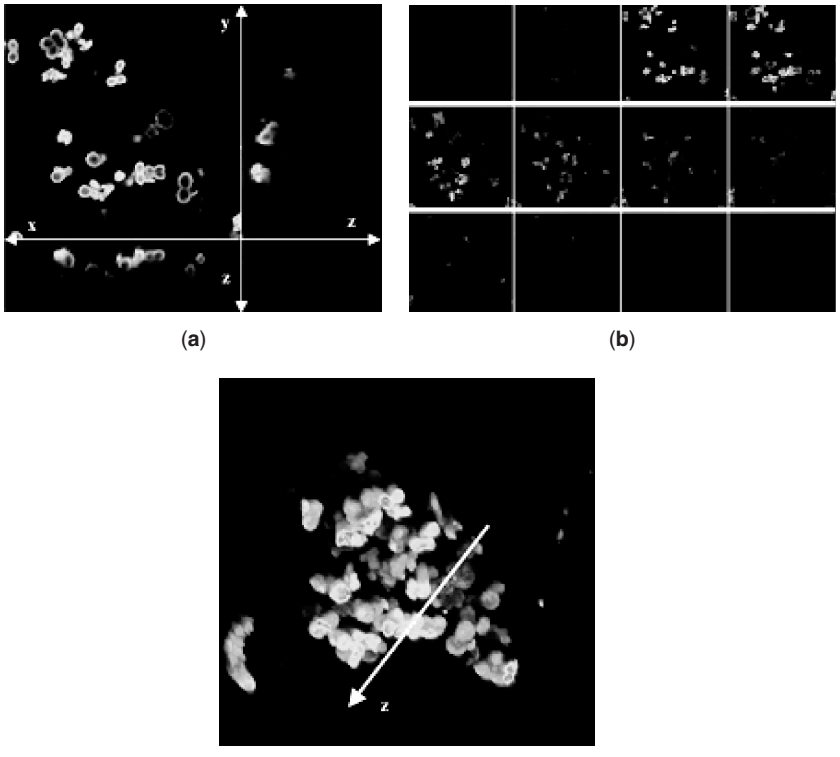

Figure 4. Three-dimensional optical sectioning of fluorescently labeled polyelectrolyte nanocapsules (15). (a) Axial and side views of the sample. (b) *xy*-slices at different focusing depth. (c) 3-D rendering of the sample. (This figure is available in full color at http://www.mrw.interscience.wiley.com/ebe.)

the several numerous current and potential applications (7–9,16). Also, the fast advances in setup are bringing confocal microscopy to a wider arena of applications, two of them are fast scanning systems that allow one to break the 2-ms-per-line temporal barrier (17) and special setup for endoscopy that permit launching confocal imaging in the human body (18,19). Most common applications of confocal microscopy are related to (1,16,17) (1) producing optical slices of transparent fluorescent specimens for 3-D reconstruction, stereo image production and four-dimensional imaging (20–24); (2) tracing specific molecules, cells, or structures through tissues (25–27); and (3) determining the cellular localization of ions, RNA, DNA, proteins, cytoskeletal components, and organelles (1,6). Many other applications can be found in literature; the Masters' volume on *Selected Papers on Confocal Microscopy* (28) can be used as an effective starting point. Moreover, confocal microscopes can also be used in the reflectance mode with applications on quality analysis of semiconductor devices (29). In terms of applications, the advent of the so-called green fluorescent proteins (GFPs) (30) and quantum dots (QDs) (31) coupled to original approaches like FRAP (fluorescence recovery after photobleaching), FRET (Fortser-fluorescence resonance energy transfer), FLIM (fluorescence life-time imaging), and FCS (fluorescence correlation spectroscopy), also known as "F" techniques, is adding value to confocal microscopy, allowing one to get quantitative information from the very complex, intricate, and delicate world of biological systems (32,33).

6. CONCLUSION

Confocal microscopy can be considered one of the most significant advances in optical microscopy within the last decades, and it has become a powerful investigation tool for the molecular, cellular, and developmental biologist; the materials scientist; the biophysicist; and the electronic engineer. It is entirely compatible with the range of "classic" light microscopic techniques and, at least in scanned beam instruments, can be applied to the same specimens on the same optical microscope stage.

Its peculiar advantages result in its ability to generate multidimensional (*x-y-z-t*) images by noninvasive optical sectioning with a virtual absence of out-of-focus blur, its ability for multiparametric imaging of multiple labeled samples, and its property of investigating at microscopic resolution large objects, thanks to the rejection of scattered light. One fundamental step in multiparametric imaging, including "F" techniques, came from the introduction of precise spectral confocal heads several years ago (34). The relevance of such an approach implemented for the first time in the Spectral Leica confocal microscopes by means of a simple but effective optical prism can be evidenced by the fact that nowadays all confocal microscopes introduce spectral channels that are endowing confocal microscopy of a fifth dimension, the spectral one. A sort of natural evolution of confocal microscopy is given by the introduction of two-photon excitation microscopy (7,35) as shown in the MULTIPHOTON MICROSCOPY article of this book.

BIBLIOGRAPHY

1. A. Periasamy, ed., *Methods in Cellular Imaging*. New York: Oxford University Press, 2001.
2. J. P. Robinson, *Current Protocols in Cytometry*. New York: Wiley, 2001.
3. A. Diaspro, ed., New world microscopy. *IEEE Eng. Med. Biol. Mag.* 1996; **15**(1):29–100.
4. T. Wilson and C. J. R. Sheppard, *Theory and Practice of Scanning Optical Microscopy*. London, U.K: Academic Press, 1984.
5. M. Minsky, Memoir of inventing the confocal scanning microscope. *Scanning*. 1998; **10**:128–138.
6. S. V. Paddock, ed., *Methods in Molecular Biology, Vol. 122: Confocal Microscopy, Methods and Protocols*. Totowa, N.J: Humana Press, 1999.
7. A. Diaspro, ed., *Confocal and two-photon microscopy: Foundations, applications, and advances*. New York: Wiley-Liss, 2002, 1–576.
8. C. J. R. Sheppard and D. M. Shotton, *Confocal Laser Scanning Microscopy*. Oxford, U.K.: BIOS Scientific Publishers, 1997.
9. J. B. Pawley, ed., *Handbook of Biological Confocal Microscopy*, 2nd ed., New York: Plenum Press, 1995.
10. D. A. Agard, Optical sectioning microscopy: Cellular architecture in three dimensions. *Annu Rev Biophys.* 1984; **13**: 191–219.
11. T. Wilson, ed., *Confocal Microscopy*. London, U.K.: Academic Press, 1990.
12. M. Born and E. Wolf, *Principles of Optics*, 6th ed., Oxford: Pergamon Press, 1993.
13. A. Diaspro, S. Annunziata, and M. Raimondo, Three-dimensional optical behaviour of a confocal microscope with single illumination and detection pinhole through imaging of subresolution beads. *Microsc. Res. Tech.* 1991; **45**:130–131.
14. A. Diaspro and F. Federici, Influence of refractive-index mismatch in high-resolution three-dimensional confocal microscopy. Appl. Opt. 2002; **41**(4):685–690.
15. A. Diaspro, S. Krol, O. Cavalleri, D. Silvano, and A. Gliozzi, Microscopical characterization of nanocapsules templated on ionic crystals and biological cells toward biomedical applications. *IEEE Trans. Nanobiosci.* 2002; **1**(3):110–115.
16. B. Matsumoto, *Cell Biology Applications of Confocal Microscopy*. San Diego, CA: Academic Press, Elsevier Inc., 2002.
17. R. D. Goldman and D. L. Spectro, eds., *Live Cell Imaging: A Laboratory Manual*. Cold Spring Harbor Laboratory Press, 2004.
18. T. F. Watson, M. A. A. Neil, R. Juskaitis, R. J. Cook, and T. Wilson, Video-rate confocal endoscopy. *J. Microsc.* 2002; **207**:37–42.
19. J. A. Evans and N. S. Nishioka, Endoscopic confocal microscopy. Curr. Opin. Gastroenterol. 2005; **21**(5):578–584.
20. G. J. Brakenhoff, H. T. van der Voort, E. A. van Spronsen, W. A. Linnemans, and N. Nanninga, Three-dimensional chromatin distribution in neuroblastoma nuclei shown by confocal scanning laser microscopy. *Nature.* 1985; **317**(6039): 748–749.
21. A. Diaspro, F. Beltrame, M. Fato, and P. Ramoino, Characterizing biostructures and cellular events in 2D/3D [using wide-field and confocal optical sectioning microscopy]. *IEEE Eng. Med. Biol. Mag.* 1996; **15**:92–100.
22. A. Diaspro, S. Annunziata, M. Raimondo, and P. Ramoino, A single-pinhole confocal laser scanning microscope for 3-D

imaging of biostructures. *IEEE Eng. Med. Biol. Mag*. 1999; **18**:106–100.

23. F. Beltrame, A. Diaspro, M. Fato, P. Ramoino, and I. Sobel, Optical sectioning microscopy and bioimage-oriented interfaces for 2D/3D and time-variant characterization of biostructures. *Engineering in Medicine and Biology Society, IEEE 17th Annual Conference*, Vol. 1, 1995: 503–504.
24. F. Beltrame, A. Diaspro, M. Fato, I. Martin, P. Ramoino, and I. E. Sobel, Use of stereo vision and 24-bit false-color imagery to enhance visualization of multimodal confocal images. In: T. Wilson and C. J. Cogswell, eds., *Three-Dimensional Microscopy: Image Acquisition and Processing II Proc. SPIE*. 1995; **2412**:222–229.
25. T. Ota, H. Fukuyama, Y. Ishihara, H. Tanaka, and T. Takamatsu, In situ fluorescence imaging of organs through compact scanning head for confocal laser microscopy. *J. Biomed. Opt*. 2005; **10**(2): 024010.
26. A. Demuro and I. Parker, Optical single-channel recording: imaging Ca2+ flux through individual ion channels with high temporal and spatial resolution. *J. Biomed. Opt*. 2005; **10**(1):11002.
27. T. Hama, A. Takahashi, A. Ichihara, and T. Takamatsu, Real time in situ confocal imaging of calcium wave in the perfused whole heart of the rat. *Cell Signal*. 1998; **10**(5): 331–337.
28. B. R. Masters, *Selected Papers on Confocal Microscopy*. Bellingham, WA: SPIE Press, 1996.
29. J. J. Miranda and C. Saloma, Four-dimensional microscopy of defects in integrated circuits. *Appl. Opt*. 2003; **42**:6520–6524.
30. R. Y. Tsien, Breeding molecules to spy on cells. *Harvey Lect*. 2003–2004; **99**:77–93.
31. J. K. Jaiswal, E. R. Goldman, H. Mattoussi, and S. M. Simon, Use of quantum dots for live cell imaging. *Nat. Methods*. 2004; **1**(1):73–78.
32. J. Lippincott-Schwartz, E. Snapp, and A. Kenworthy, Studying protein dynamics in living cells. *Nat. Rev. Mol. Cell Biol*. 2001; **2**(6):444–456.
33. J. W. Dobrucki, Confocal microscopy: Quantitative analytical capabilities. *Methods Cell Biol*. 2004; **75**:41–72.
34. R. Borlinghaus, Benefits and applications of programmable spectral devices in confocal microscopes. *Proc. SPIE*. 2003; **4964**:7–13.
35. W. Denk, J. H. Strickler, and W. W. Webb, Two-photon laser scanning fluorescence microscopy. *Science*. 1990; **248**(4951): 73-76.